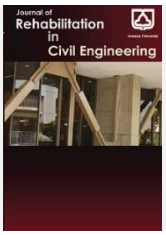

Journal of Rehabilitation in Civil Engineering

Journal homepage: https://civiljournal.semnan.ac.ir/

Development of a New Modified Sonar Inspired Optimization based on Machine Learning Methods for Evaluating Compressive of High-Performance Concrete

Ali Nikkhoo [1*]; Amin Moshtagh [2]; Mehri Mehrnia [3]

1. Associate Professor, Faculty of Engineering, University of Science and Culture, Tehran, Iran
2. Ph.D. Student, Department of Civil Engineering, University of Science and Culture, Tehran, Iran
3. Ph.D. Student, Department of Biomedical Engineering, Northwestern University, United States

Corresponding author: *nikkhoo@usc.ac.ir*

ARTICLE INFO

Article history:
Received: 16 March 2024
Revised: 17 April 2024
Accepted: 29 April 2024

Keywords:
High-performance concrete;
Sonar inspired optimization;
Optimization;
Artificial neural network;
Prediction.

ABSTRACT

The nonlinearity observed in high-performance concrete (HPC) can be attributed to its distinctive features. This study examines the effectiveness of expert frameworks in determining compressive strength, aiming to enhance accuracy through the development of a master artificial neural network (ANN) system utilizing the sonar inspired optimization (SIO) algorithm. The ANN model employs exploratory data to establish initial optimal weights and biases, thereby improving precision. Comparison with previous studies validates the accuracy of the proposed system, demonstrating that the SIO-ANN hybrid model offers finer estimation of high-performance concrete properties. Results consistently show a coefficient of determination (R^2) exceeding 0.972 and a 50%-67% reduction in error rates compared to conventional fitting curve approaches. Parameters such as population, weight, and bias within the SIO-ANN framework are continuously updated and optimized to achieve optimal values efficiently. Additionally, the SIO-ANN model exhibits superior runtime performance compared to other models. Consequently, the proposed SIO-ANN approach emerges as a viable alternative for accurately assessing and predicting the compressive strength of high-performance concrete.

E-ISSN: 2345-4423

How to cite this article:
Nikkhoo, A., Moshtagh, A., & Mehrnia, M. (2024). Development of a New Modified Sonar Inspired Optimization based on Machine Learning Methods for Evaluating Compressive of High-Performance Concrete. Journal of Rehabilitation in Civil Engineering, 12(4), 116-135. https://doi.org/10.22075/jrce.2024.33564.2025

1. Introduction

Recent advancements in civil engineering have seen a rise in High-Performance Concrete (HPC) use for structures like skyscrapers, high-speed railways, and massive bridges. These structures need to withstand extreme forces like explosions, impacts, and fires. HPC offers several advantages over traditional concrete, including superior strength, flexibility, and resistance to water penetration [1–7]. To achieve this enhanced strength, engineers incorporate additional materials like nano-silica, silica fume, and industrial byproducts like blast furnace slag and fly ash into the concrete mix [6–10]. Nonetheless, HPC properties rely upon numerous components, for instance, blend extents, quality of used material, and cement age [11]. Subsequently, estimating HPC's compressive and tensile strength is a fundamental assignment since it can assist with planning tasks in the beginning phases of the underlying model, decreasing exploratory necessities. Hence, an exact strategy to predict HPC's compressive strength is able to fundamentally lessen time and expenses. Numerous scientists have utilized simulation methods based on mechanics to evaluate the cement strength [12–16]. Rabczuk et al. displayed the fracture of a few strengthened solid constructions through a three-dimensional strategy, which has no mesh [15]. Rabczuk and Belytschko used particle strategies to find a solution for a few fracture issues, including strengthened solid constructions, and the computational outcomes demonstrated great concurrence with exploratory information [14]. Rabczuk et al. suggested a 2D method to simulate the fracture in structures consisted of reinforced concrete and considered the correlation between the reinforcement and the concrete [16]. Drzymałaa utilized a trial technique to explore the impacts of high temperatures on HPC characteristics [17]. In a preliminary study, Zhao et al. [18] examined how fly ash and ground granulated blast-furnace slag affect shrinkage in High-Performance Concrete (HPC). Moreover, a few techniques have been performed to discover the correlation between the critical items that may impact HPC's compressive strength, for example, cement, superplasticizer, fly ash, water, and testing age [19]. Be that as it may, achieving an exact regression function is very difficult using these techniques as HPC's compressive strength is influenced by numerous elements. Likewise, the concrete properties have an exceptionally nonlinear correlation with its components, which presents challenges in figuring HPC's compressive strength from accessible information [20]. Subsequently, the standard strategies utilized for ordinary concrete are frequently unacceptable for determining HPC's compressive strength.

Much Artificial intelligence (AI) procedures were suggested to obtain a solution for the mentioned problem [21–35]. Chou and Pham acquainted new computing models to predict HPC's compressive strength [36]. This model was made by joining numerous AI strategies. Prasad et al. utilized an ANN model to estimate HPC and self-compacting concrete [37]. Naderpour et al. focused on reused aggregate concrete, using a technique called ANN for estimating the compressive strength [38]. In another study, Ali et al. employed a tree algorithm to estimate the compressive strength of both regular concrete and HPC [39]. The association between the variables' input and output is ignored in AI methods. Furthermore, the trained data's input parameters ought to cover the input of the estimative data that is a weakness of these models [40]. These are largely encouraging methodologies, yet they are profoundly reliant on the initial parameters that are a solid limitation that restrains the function. Subsequently, these AI procedures should be joined with optimization algorithms [41]. Several researchers have proposed using

machine learning models to solve problems in various fields of engineering. For example, Nazari and Sanjayan improved a method called Support Vector Machine (SVM) to better estimate the compressive strength of mortar, geopolymer, and concrete [42]. Their approach involved using five different optimization algorithms to fine-tune the SVM's parameters. In another study, Marek employed a combination of neural networks and Bayesian statistics to predict the compressive strength of HPC. The firefly algorithm is an effective optimization instrument among numerous optimization algorithms applied to enhance the performance of machine learning techniques in several research cases. Chou et al. solved numerous civil engineering estimation problems using least square support vector regression based on the firefly algorithm [43]. Ibrahim and Khatib [44] applied the firefly algorithm to estimate the global solar radiation in an hourly manner to optimize the random forests technique. Nonetheless, utilizing the FA for improving the capacity of ANN has not gotten much consideration, particularly in civil engineering. The purpose of this research is to optimize the ANN weights and biases to better estimate HPC's compressive strength using modified firefly algorithm. The chaotic map and Lévy flights components were combined with the firefly algorithm to achieve a high dimensional optimization. Besides, SIO updated, retained, and optimized the ANN parameters during the training, which dramatically reduced the computing time. This examination additionally expects to confirm the master system by utilizing a k-fold cross-validation algorithm. Then, the hypothesis testing was conducted to compare the SIO-ANN performance with different strategies utilized in similar studies [45–47]. Then, the paper was presented in five parts. The following part provides a review of the research subject regarding the estimation of HPC compressive strength through machine learning techniques. The third part depicts the exploration procedure and execution assessment techniques. The fourth part blueprints the characteristics that influenced the HPC compressive strength and two test datasets utilized in this research. The fifth part consequently shows the preprocessing of data, the application of the model, the estimation of the SIO-ANN results, and checks the model's function compared to different techniques dependent on the results. The last part will sum up the study and give concluding up comments.

2. Literature review

Compressive strength is a critical undertaking in civil engineering given because of needing numerous inputs from different design rehearses [48,49]. Having a reliable model that can accurately predict the compressive strength of materials early in a project can shorten the overall project timeline [49]. Lately, numerous examinations utilizing different methodologies for assessing the strength of concrete have been accounted [50–54]. AI was previously proved to work well in construction materials description [55,56,65,57–64]. Erdal [66] estimated the HPC compressive strength with two-section and mixed ensembles for decision trees. This study proposed three different ways to combine machine learning models (ensemble methods). These methods included using multiple decision trees, combining two separate models, and a combination of both approaches. The results showed that these combined models were significantly more accurate at predicting the compressive strength of HPC compared to using a single model. Yuvaraj et al. [67] inspected the pertinence of SVM to estimate the fracture attributes of concrete beams at high strength and ultra-high-strength levels. According to results, SVR could get comparative outcomes with those from tests. Yeh [20] showed the prospects of utilizing ANN to estimate HPC's compressive

strength. Accordingly, acquired more precise outcomes than a model dependent on regression-based analysis. ANN was able to review the impacts of every concrete mix ingredient as numerical experiments. Moreover, Sobhani et al. estimated no-slump concrete's compressive strength by comparing ANN models and fuzzy systems based on an adaptive network [51]. This study found that ANNs were a more effective way to predict the compressive strength of concrete that doesn't flow easily (no-slump concrete) after 28 days, compared to traditional mathematical models [68]. To improve the performance of ANNs, researchers have explored various optimization algorithms. One example is the work of Lee et al., who used a technique called the harmony search algorithm to find the best starting values for the weights in the ANN during the training process [68]. Alavi and Gandomi presented estimated the ANN optimal initial coefficients by simulating annealing techniques [69]. Chang et al. found the optimal weights to increase the precision of ANN using genetic algorithms [70]. Liu et al. executed the ensemble technique to increase the exactness of the basic model [71]. The mentioned types of research confirmed the high-performance of hybrid models in solving problems. However, a few examinations utilized hybrid models explicitly, ANN-based firefly algorithm (FA) to estimate HPC's compressive strength. This algorithm achieved a better performance as an optimization algorithm in many types of research [28,72]. Moghaddam et al. estimated the polyethylene terephthalate's fatigue life changed asphalt mixtures using an FA-based support vector machine [72]. Kazemivash and Moghaddam assessed digital image watermarking using a regression tree with the help of FA [73]. Subsequently, this investigation utilized SIO-ANN to estimate HPC's compressive parameter through the 10 cross-fold validation and multi-function criteria to fix this problem. According to comparisons, the hybrid master system had a finer precision with minimum computational expenses.

3. Methodology

3.1. Dataset

Published datasets were used to assess the efficiency of the suggested master system [74–78]. Dataset incorporates 1133 samples of HPC with 1 output variable and 8 inputs variables. The amount of cement (X1), blast furnace slag (X2), water (X3), fine aggregate (X4), coarse aggregate (X5), fly ash (X6), superplasticizers (X7), and the testing age (X8) were the eight inputs, and the compressive strength (Y) was the output. The concrete's compressive strength was affected by each input parameter. For instance, Johnson and Bawa indicated that the ratio of fixed water test to cement was increased by the compressive strength [79]. The density of concrete will be increased by an expanding aggregate-cement ratio, which affects the compressive strength, as well as the dynamic modulus [79]. Moreover, the impact of each independent on the output ought to be researched. For example, Vu-Bac et al. quantified the input parameters' influence on uncertain outputs using a software framework [80]. Hamdia et al. assessed the input parameters' sensitivity through a polynomial model [81]. Also, the concrete compressive strength is affected by many other parameters, such as formation, slump, and curing conditions. Be that as it may, the research's primary purpose is to assess the presentation of the suggested SIO-ANN in assessing HPC's compressive strength. Consequently, the investigation utilizes similar 8 inputs, 1 output, and some datasets to acquire fitting correlations. Fig. 1 provides 8 scatter plots for all inputs.

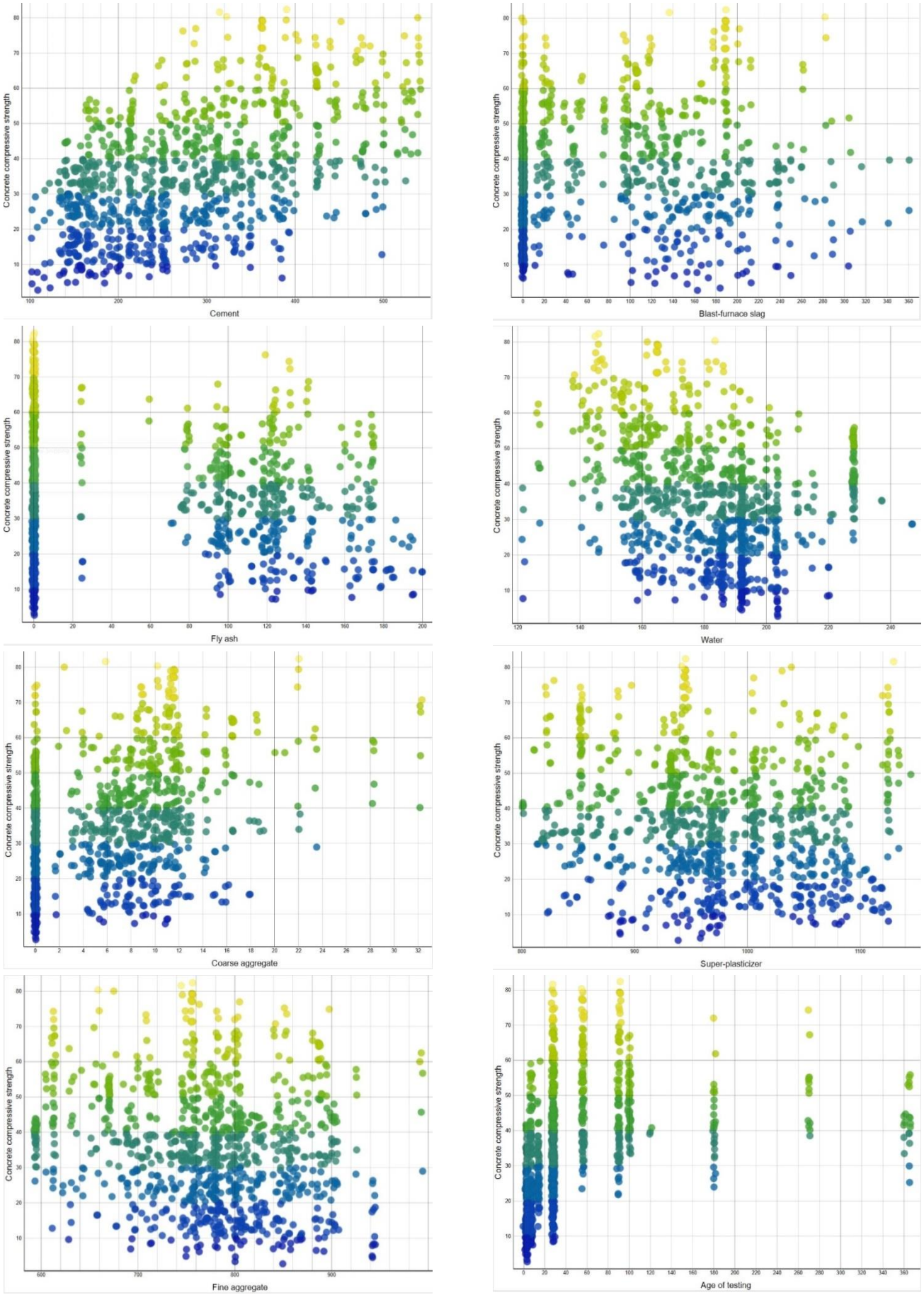

Fig. 1. The scatter plot of all data.

3.2. Machine learning models

ANNs are inspired by the structure and function of the human brain. Similar to how our brains work with interconnected neurons, ANNs rely on a network of interconnected units called artificial neurons (Fig. 2). Neuron transmit signals to each other through a synapse or a weighed connection that can alter the strength of the signal [31,82,83]. The development of ANN is separated into three fundamental advances:

a) Characterizing inputs and outputs;

b) Optimizing the structure by altering the layers' weights and bias; and

c) Examining the network function by contrasting the estimated and actual values.

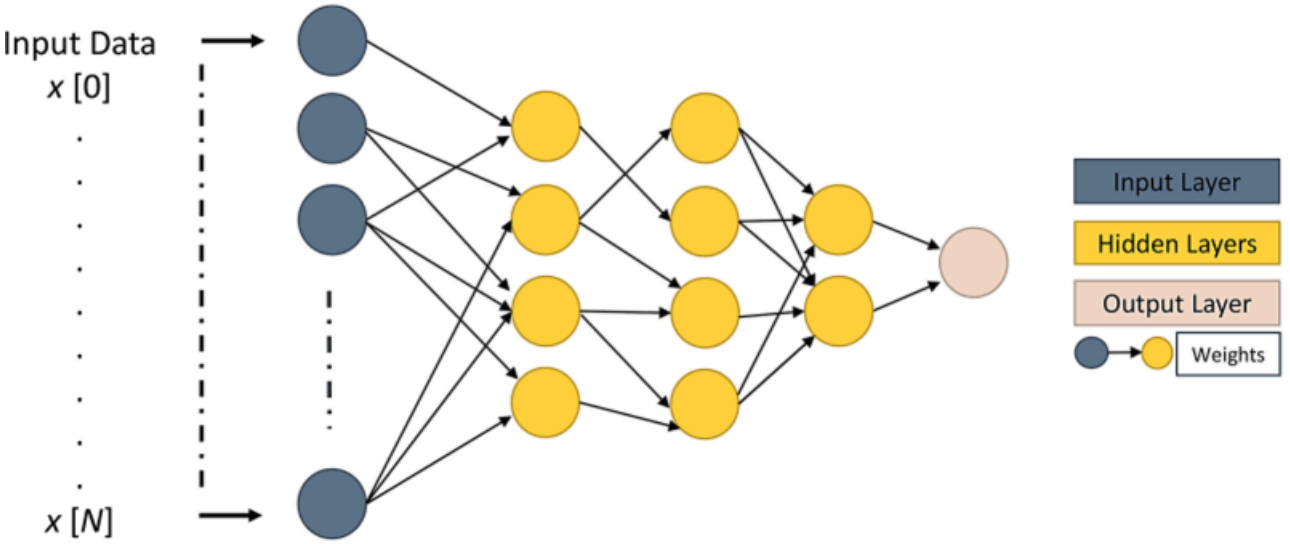

Fig. 2. The structure developed for the present study.

Eq. (1) is a linear function, which calculates the sent signals to the hidden nodes from the inputs depending on input weights and bias before going to a transfer function to obtain the target of the hidden node [84].

$$net_i = \sum_{i=1}^{8} w_{i,j} I_j + b_i \quad (1)$$

This describes the calculations within an ANN. Here, 'neti' represents the sum of weighted inputs to a specific hidden neuron (i). Each input from another node (j) is multiplied by its corresponding weight (wi,j) and then summed. An additional bias parameter (bi) is also included for the hidden neuron. This research uses a mathematical function called the sigmoid function (see Equation (2)) to process this combined value (neti) within the hidden neuron.

$$y_i = f(net_i) = \frac{1}{1+\exp(-net_i)} \quad (2)$$

In which, y_i is the ith hidden node output signal; exp (-net_i) is Euler's number to the net_i power. The training process was evaluated by the mean square error as the objective function. The actual error (€) is calculated using a formula that will be explained next:

$$E = \frac{1}{N \times N_{out}} \sum_{n=1}^{N} \sum_{o=1}^{Nout} (e_{n,o})^2 \quad (3)$$

In which, $e_{n,o} = \bar{y}_{n,o} - y_{n,o}$ is the training error of output o in the case of applying instance n; n is the training instance index; N is the instance number; o is the output index, Nout is the output number; $\bar{y}$ is the estimated data by ANN, and y is the real data. Then, the bias and weights parameters are changed to reduce the error E to the minimum level through the learning process. This research uses a specific method called the Levenberg-Marquardt algorithm [85,86] to train the ANN. This algorithm has been modified for this particular

application, and the details of the modifications are provided below:

$$W^{k+1} = W^k - (J^{k^T} J^k + \mu \bar{I})^{-1} J^{k^T} e^k \quad (4)$$

In which, 1 > 0 is the coefficient of combination; I is the matrix of identity; w^k is the matrix of weight at kth repetition, and w is a dimension vector W ×1, with the total weight number of W; wk+1 is the matrix of weight at (k + 1)th repetition, and The Jacobian matrix (J), mentioned in the reference source [87], likely plays a role in calculating the adjustments to the weights..

3.3. Optimization

3.3.1. The actual sonar mechanism

The main concept this mechanism is the utilization of a sonar system by warships for detection of submarines [88]. The sonar device releases an ultrasound wave to strike an object and back-propagate. The wave after reflection by the target is received by the sonar system, by help of which the size of the object can be estimated and the crew of warship can easily detect the location of the target (refer to Fig. 3).

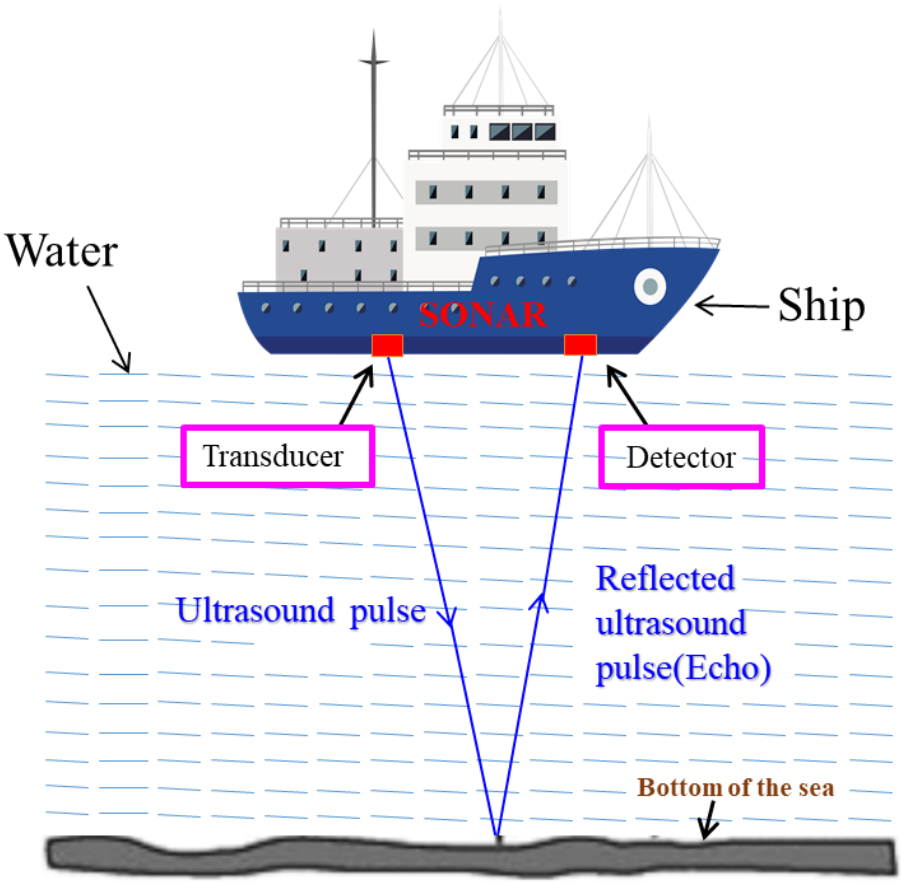

Fig. 3. Sonar mechanism in a schematic view.

The sonar system periodically submits waves to the environment surrounding the warship. Intensity of sound is realized so as to provide a modeling of the mentioned event [89]. To this end, we need to find the Acoustic Power Output or Sound Power (P):

$$P = \eta . P_e \quad (5)$$

In the above equation, P_e denotes the input power and η shows the efficiency of the transducer. The latter parameter is calculated by dividing the output power to the input power and is expressed in percent. Once P is found, the following equation is used to obtain the intensity of sound which is defined by dividing P over the surveyed area (refer to Fig. 4):

$$I = \frac{P}{area} \quad (6)$$

The scanned area is obtained by:

$$area = 4.\pi.r^2 \quad (7)$$

where, r shows the radius of the imaginary sphere (area) surveyed by the sonar system.

It can be seen that if the value of intensity (I) is decreased the effective radius r will increase. The suggested method in this work has also employed this equation.

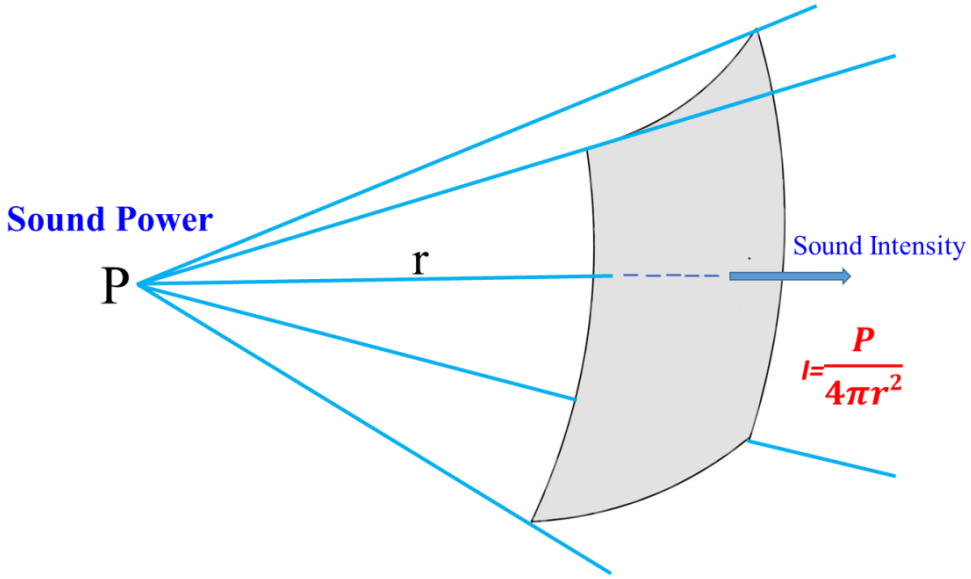

Fig. 4. The relationship between sound power and sound intensity.

3.3.2. The proposed SIO algorithm

Individual agents given in Xi = {x1, x2, x3, …, xn} (i ϵ 1, 2, …, N), where N = the maximum number of agents and n represents the maximum dimensions of problem. The ship number is initially determined to save computational power. In general, if the number of agents is big, the probability of reaching the optimal solution will increase. Nevertheless, this is not true for the suggested algorithm [88]. According to the following subsections, the mass of points produced in the vicinity of individual agents yields a wider solution space without manipulating the number of agents. One significant advantage provided by the presented method is that the space within which the solution is searched is wide enough to maintain the number of agents. Initially, the positions of agents are randomly selected within the solution space. One straightforward technique to accomplish this is to utilize the normal distribution function. Yet, the positions can be changed with regard to the values each of the decision variables can adopt. The initial radii and intensities of individual agents are found according to Eqs. (6) and (7). The input power is set as the fitness of agents:

$$Pe = fit_i, i \in \{1,2,\dots,N\} \quad (8)$$

Also, Eq. (8) can be rewritten to turn the fitness values into positive quantities:

$$P = e^{Pe} \quad (9)$$

This task is a necessity as a logarithm function is used for changing the scale of intensities. Logarithm functions cannot take negative values, but fitness values can take negative values in specific problems. Therefore, this issue is tackled in this work using a transformation inspired by a physical interpretation. The maximum number of iterations, here called “number of scans” has been adopted is the termination criterion in the experiments performed. The fitness function values are found for each of the warships to reach the best answer. The best answer is

recorded and all agents alter their intensities concerning the answer already obtained. In the case the new answer is better than the previous one, the intensity is increased; otherwise, it is decreased. Thus, the effective radii are correspondingly changed. In the end, the proposed method adopts another mechanism. Practically, if no suspicious object is detected by the warship, the ship leaves that region. One simple approach to change the location of an agent is to consider the position of the best answer attained hitherto:

$$x_i^d = best^d + r_0^i.rand \quad (10)$$

Here, x_i^d represents the location of agent number ith on a specific dimension (d). $best^d$ refers to the most favorable position found so far in the current round. r_0^i indicates the effective search area (radius) for agent 'i'. Finally, 'rand' is a random number chosen uniformly, meaning it has an equal chance of being any value within a specific range. Nonetheless, we can rewrite the above equation to change the location of an agent in areas that have not been searched up to this point. Using a comparable concept of the mutation rate [90]:

$$\mu_{opt} = \frac{1}{\tau} \quad (11)$$

where, μ_{opt} represents the interval between significant environmental changes.

3.3.3. Intensity parameter

Intensity is the most significant parameter in the proposed algorithm and impacts the variations of the effective radius and, consequently, the maximum area the agents search. Definition of this parameter is updated after each iteration according to the solution achieved by the corresponding agent:

$$I_i = I_i.e^{magnitude} \quad (12)$$

By defining magnitude we can indicate the significance of the target detected by the agent/warship. A definition of magnitude is given here:

$$magnitude = scan\_best_i - best + s \quad (13)$$

In this equation, $scan\_best_i$ denotes the fitness of the best solution achieved by the ith agent in the current scan and best represents the best global solution obtained so far. A trivial value (s) is also added to the previous terms so as to prevent a zero magnitude for the agent with the global best solution. Equations 13 is written according to the graph of e^x referring to Fig. 5, in the case x for e^x is smaller than zero, y is smaller than one. The intensity level helps agents adjust their search behavior. When the agent finds a solution that's better than its previous one (negative magnitude), the intensity decreases. This encourages the agent to take smaller steps and refine its search around the improved solution. Conversely, if the agent finds a worse solution (positive magnitude), the intensity increases. This pushes the agent to explore further and potentially take larger steps to find a better solution. Furthermore, the farther the optimal solution is, the greater the increase in intensity. This means the agent will make bigger jumps in its search when it's far away from the ideal solution, gradually adjusting its steps as it gets closer.

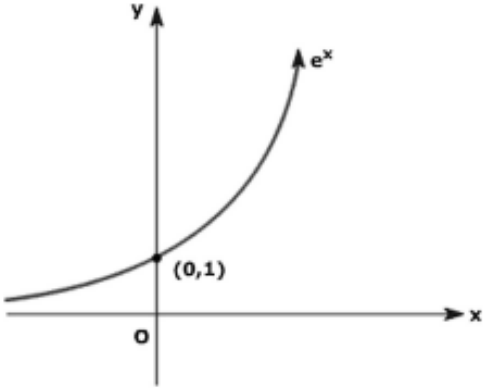

Fig. 5. The defined function for intensity parameter.

The following equation is used to turn the high value of Ii into a helpful value by realizing a physical analogue:

$$I_i = 10.\log\frac{I_i}{I_0} \quad (14)$$

here, Ii shows the intensity of the ith agent and I0 represents the Threshold of Hearing [89] as follows:

$$I_0 = \frac{10^{-12} watts}{m^2} = 10^{-16} watss/cm^2 \quad (15)$$

In the conducted experiments, we set the value of I_0 equal to 10-12, although we can vary the value based on the problem under study.

3.3.4. Effective radius (r_0)

The solution space determines the initial value of r0. The algorithm takes smaller steps if r_0 is a small value. By the same token, for larger values of radius, there will be larger jumps in the algorithm towards reaching better optima. However, in the latter case, potential solution might be missed. The effective radius can be found via reversing Eq. (16):

$$r_0 = \sqrt{\frac{area_i^k}{4.\pi}} \quad (16)$$

where, $area_i^k$ gives the area analyzed by the ith agent in the kth iteration. The provided model reveals the actual relationships among the measures. For larger values of intensity, the scanned area is larger than that obtained for lower values of intensity. As a result, the effective radius will be smaller as well. We try to increase the value of r_0. In the case no better solution is achieved, agents should search farther areas.

3.3.5 Full Scan Loop

To explore more of the possible solutions, agents use a technique called the Full Scan Loop. In each round (iteration), agents investigate their surrounding area, limited by their effective search radius (r_0). The name "Full Scan Loop" reflects the repetitive nature of this process – agents perform three steps repeatedly until they've thoroughly searched their designated area. By starting from 0o, random rotations with maximum coverage of a^o are performed in each dimension.

$$angle^d = angle^d + rand \times a^\circ \quad (17)$$

In the above equation, rand is a random number generated by a uniform distribution function and angled represents the rotation angle in the dimension d. When angled exceeds 360o, the loop is terminated. In every dimension, the vector of angles is transformed into a vector of movements:

$$x_1^2 + x_2^2 + \cdots + x_n^d = r^2 \quad (18)$$

Here, r is the random radius inside a cycle formed by r_0 and n shows the number of dimensions of the problem. Fig. 6 illustrates an example of 36 points explored in a single dimension for a mathematical function called Ackley's function. This approach allows each agent to investigate multiple points around its current location simultaneously. In contrast, some other algorithms limit each agent to examining only one point per round. The new position is found by:

$$x_i^d = movement^d + x_i^d \quad (19)$$

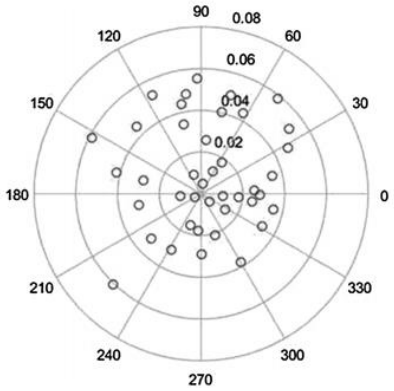

Fig. 6. A sample of points generated for the Ackley's function.

where, xid shows the position of the ith agent in the dth dimension and movementd represents the dth element in Eq. 20. In each rotation phase, the fitness value of the new one is computed. A correction procedure has also been carried out to prevent violating the acceptable range of possible solutions. If there is a x_i^d that violates the bound constraints, its new location will be calculated by:

$$x_i^d = lower\_bound^d + (upper\_bound^d - lower\_bound^d).\cos(x_i^d) \quad (20)$$

so that the inequality lower_bound^d < xid < upper_bound^d is satisfied.

4. Performance evaluation

4.1. Data preprocessing

In this section, firstly, the relationship between independent and non-independent data is examined. Fig. 7 indicates all attributes of dataset. There is a strong non-linear correlation between HPC's compressive strength and these components. Accordingly, it is trying to locate HPC's compressive strength dependent on these datasets.

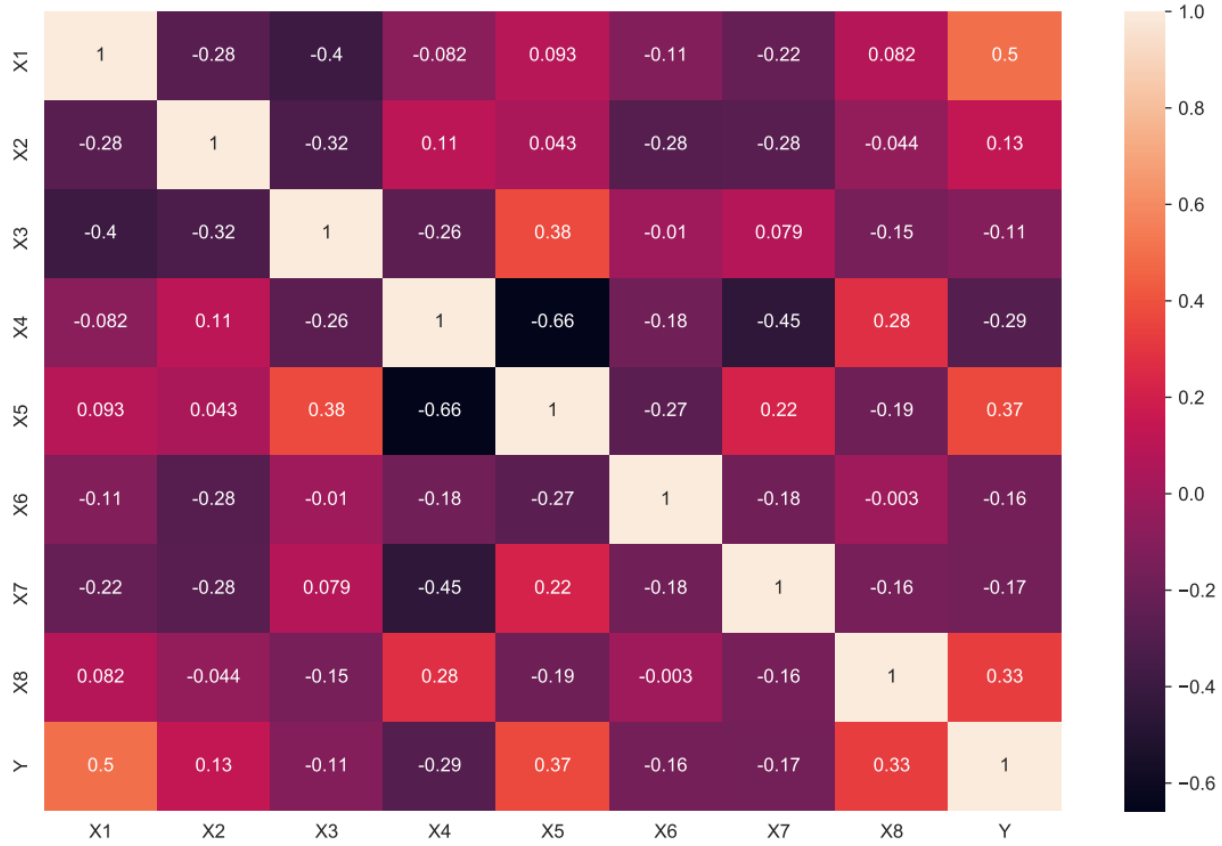

Fig. 7. The correlation matrix between all data.

The high strength concrete's compressive strength was estimated through performance tests, as well as the SIO-ANN master system. K-fold cross-validation was used to reduce errors and prevent over-fitting among models and results [91]. Some researcher showed that 10-fold is the optimal number to acquire a decent outcome inside a worthy time span [92]. Similar results are obtained by a few cross-approval strategies, for example, leave-one-out cross-approval and examining test-set cross-approval. For instance, Badawy et al. chose the most delegate training and test sample sets using the scanning test [93]. Similar to other recent research, this study employed a technique called 10-fold cross-validation to evaluate the performance of the proposed model. A total of 1133 samples are randomly elected from dataset 1 and divided into 10 particular folds to build up the framework for assessing HPC's compressive parameter. The primary fold is utilized for testing in the first validation round, while the remaining nine folds are used to train the model. This process is repeated ten times, ensuring all data points are used for both testing and training. Essentially, the folds are rotated, with each fold serving as the testing set once during the 10 rounds (Fig. 8). The model's presentation is then determined by

taking the normal execution of the ten models in ten approval rounds. A total of six cases with a restoring age of 3, 7, 28, 90, and 180 days, just as a whole dataset were evaluated. The outcomes will be contrasted and those in the past investigation. In the preprocessing step, it is critical to scale the all types of data through training ANN. A key benefit of this research is that it addresses a common issue in machine learning. When data points have vastly different numerical ranges (some values are much larger or smaller than others), it can lead to attributes with larger ranges dominating the analysis and masking the importance of attributes with smaller ranges. This study helps prevent this from happening [94]. The other advantage is to forestall numerical problems. The range of [0, 1] is used to normalize the study data utilizing the min-max normalization algorithm:

$$X' = \frac{x - \min(x)}{\max(x) - \min(x)} \quad (21)$$

Fig. 8. The process of cross validation for the current research.

The main features for the SIO-ANN hybrid technique are given in Table 1. To obtain the parameters, parametric analysis was performed for each of the parameters. Using this process, the optimal state of each was determined.

4.2. Discussion

The system function in estimating HPC's compressive is demonstrated in Table 2. The results of other studies were also compared in this section. The hypothesis test was used to validate the SIO-ANN improvement by comparing it with other methods. According to Table 2 in which reveals a lower MAE (1.801 MPa) in the suggested system rather than Multi-gene genetic programming (M-GGP) [95], Gene Expression Programming (GEP) [96], ensemble model (ANN + SVR) [36] and the Least Square Support Vector Regression based on the smart firefly algorithm (SFA-LSSVR) [43]. SIO-ANN likewise accomplishes the most reduced MAPE (5.88 MPa) and the least RMSE (2.732 MPa) contrasted with different strategies.

In general, the suggested master system's error rates are 50 %–67% finer than other studied techniques. According to hypothesis tests, SIO -ANN results are significantly (8%–20%) finer than other techniques. Additionally, SIO-ANN has a higher R^2 (0.95) esteem than different techniques (Table 2). This implies that a high potential of the relationship between the real

and target compared other in past examinations. Fig. 9 and 10 indicate the relationship between the real and target result for one case in 10-cross folds.

Table 1. The main parameters for the expert systems.

Model	Feature	Value/setting
SIO	Number of iteration	500
	Number of population	50
	Number of run	100
	The maximum rotation angle	15
	the small value s	0.00065
	d the value of Threshold of Hearing I0	10-12
	Training data	80%
	Testing data	20%
ANN	Objective function	RMSE
	Learning function	Levenberg–Marquardt
	Number of layer	1
	Number of neuron	12
	Transfer function	Tangh

Also, the processing time in running 1 repetition of cross-fold validation is significantly diminished from 15.90 min (SFA-LSSVR) to 4.10 min (SIO-ANN). Updating ANN's weight and bias parameters can lead to time improvement in the training. The regularization and the sigma parameter of the RBF kernel were optimized through the firefly algorithm in SFA-LSSVR, which are constant in the training process. In the interim, the layer weight and coefficients are updated in SIO-ANN during the ANN training process. Furthermore, the updated layer weight and coefficients parameters are restored in SIO and optimized according to them. Thus, SIO-ANN can essentially decrease figuring time running compared with chou et al. reserach [43]. Figure 11 shows a comparison between the results of different models based on Table 2, considering the two factors of R^2 and MAE. As can be seen, the SIO-ANN model has provided the highest amount of R^2 and the lowest amount of MAE for forecasting the HPC's compressive, which indicates the superior performance of this model. Figures 12 to 15 show the HPC's compressive results for different samples based on time. As can be seen, there is a high correlation for different samples with time. Due to this issue, it can be mentioned that the SIO-ANN model has been able to provide high performance in various dimensions.

Table 2. The performance of the developed model and compare its progress with previous models for the data set.

Models	Performance value				Running Time (minutes)	Improvement (%)			
	R^2	MAPE	MAE	RMSE		R^2	MAPE	MAE	RMSE
GEP	0.828	N/A	5.20	N/A	N/A	17	-	65	-
M-GGp	0.810	N/A	5.48	7.31	N/A	20	-	67	62
ANN+SVR	0.884	15.20	4.24	6.17	N/A	9.9	61	57	55
SFA-LSSVR	0.893	12.28	3.86	5.62	15.9	8.8	52	53	51
SIO-ANN	0.972	5.88	1.801	2.732	4.1	-	-	-	-

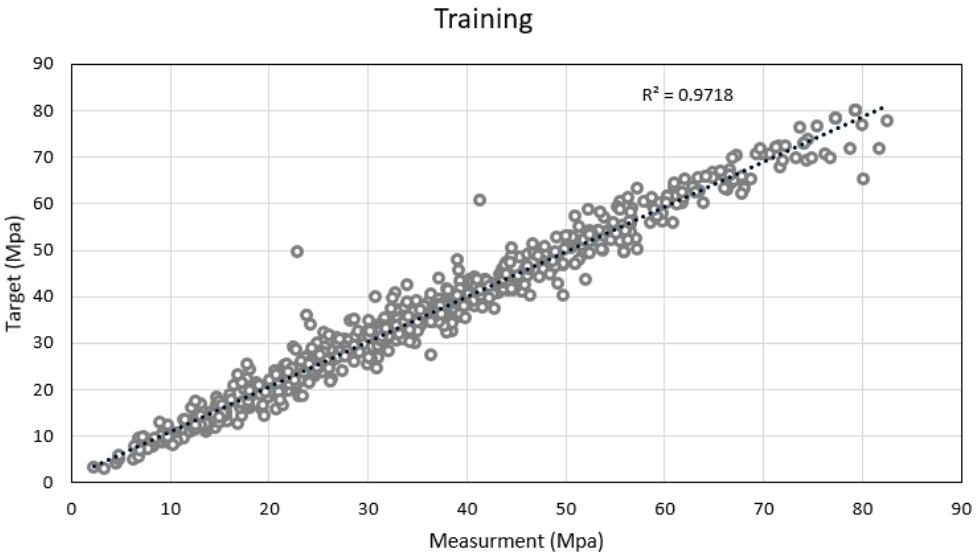

Fig. 9. Training result in estimating HPC's compressive.

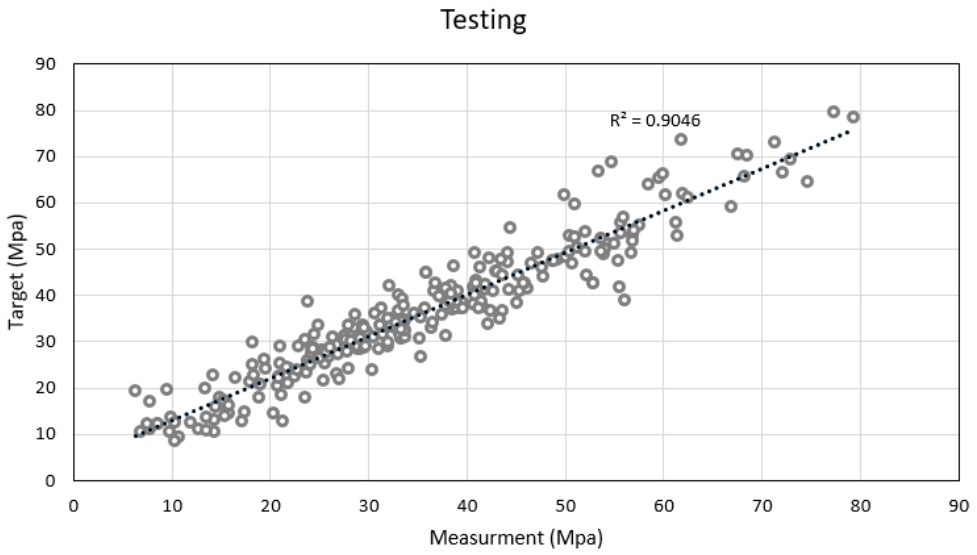

Fig. 10. Testing result in estimating HPC's compressive.

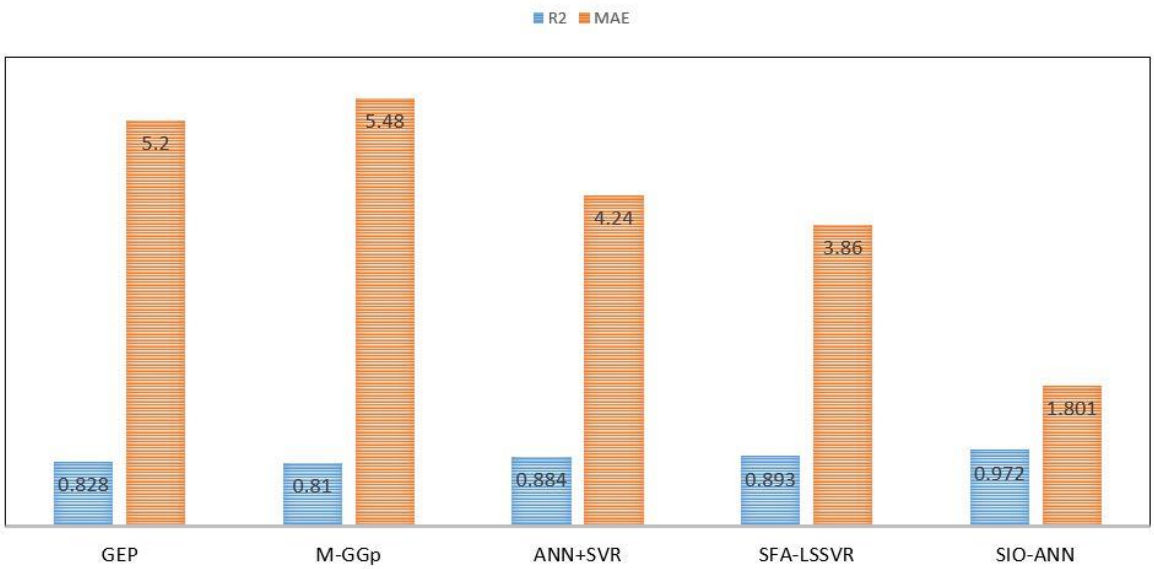

Fig. 11. A comparison between various modes based on R^2 and MAE.

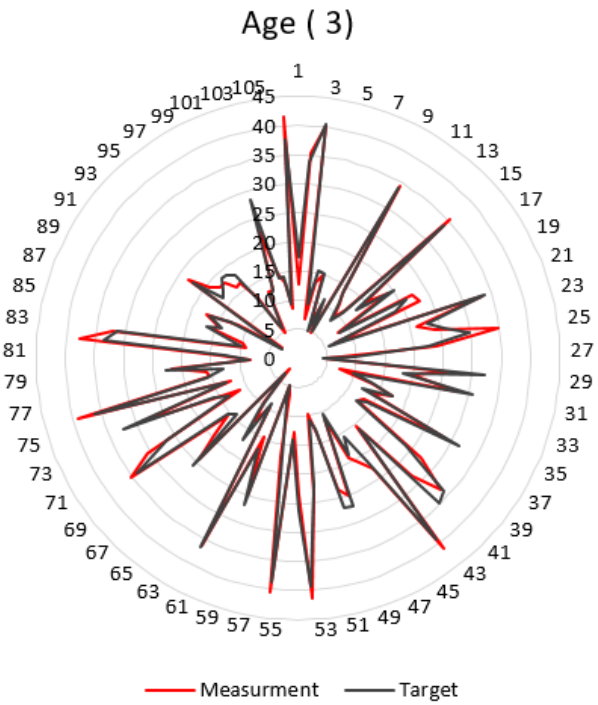

Fig. 12. The outputs of HPC's compressive for 3 days based on SIO-ANN.

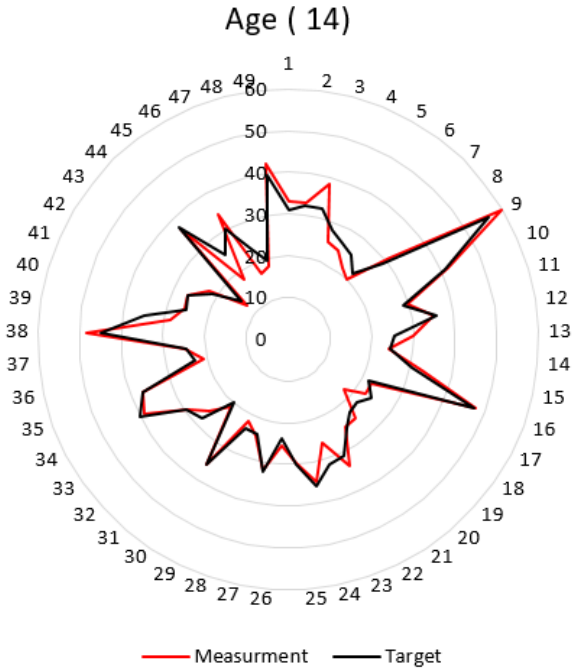

Fig. 14. The outputs of HPC's compressive for 14 days based on SIO-ANN.

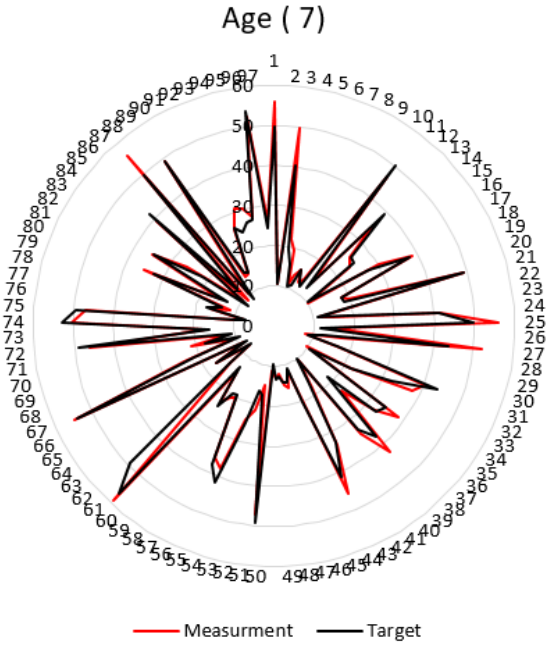

Fig. 13. The outputs of HPC's compressive for 7 days based on SIO-ANN.

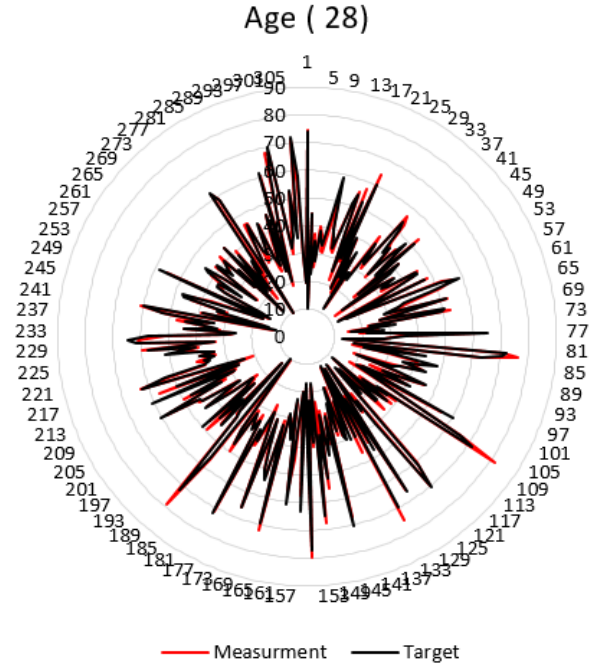

Fig. 15. The outputs of HPC's compressive for 28 days based on SIO-ANN.

5. Conclusions

A productive approach was investigated using SIO-ANN to estimate the compressive

strength of HPC for the first time. This novel methodology was evaluated using two datasets of HPC samples obtained from different laboratories, totaling 1133 cases. To address overfitting, a 10-fold cross-validation technique was employed. The accuracy of SIO-ANN in predicting HPC compressive strength was compared with various methods used in previous studies. SIO-ANN exhibited lower error rates across three error indicators compared to other techniques applied to the dataset. Additionally, SIO-ANN demonstrated a higher correlation coefficient (R^2=0.972) between actual and predicted results compared to alternative methods. The results consistently showed an R^2 exceeding 0.972, along with a 50%–67% reduction in error rates compared to the fitting curve approach. Consequently, this study confirms that the proposed framework effectively assesses HPC compressive strength and significantly reduces the need for extensive testing in the future.

The SIO-ANN hybrid model also contributed to reducing computation time. The proposed approach enhances precision and achieves nearly five times faster computation compared to the research by Chou et al. [43]. This is facilitated by constant optimization, retention, and development of parameters such as population, weight, and coefficients within the SIO-ANN framework, aiming for swift attainment of optimal values. Consequently, the proposed method offers efficient and timely estimations as a valuable tool. Additionally, this study employed a single hidden layer comprising 12 nodes. While increasing hidden layers or nodes may enhance the effectiveness of ANN training, it prolongs the optimization process for weight and bias parameters. Nonetheless, the methodology adopted in this study yielded commendable results within short processing times. Thus, the selected quantity of hidden layers and nodes proves suitable. Ultimately, the proposed approach emerges as an apt tool for rapid and accurate estimations, making it applicable to a broad spectrum of engineering challenges.

References

[1] Bezgin NÖ. High performance concrete requirements for prefabricated high speed railway sleepers. Constr Build Mater 2017;138:340–51.

[2] Ng KW, Garder J, Sritharan S. Investigation of ultra high performance concrete piles for integral abutment bridges. Eng Struct 2015;105:220–30.

[3] Nguyen KTQ, Ngo T, Mendis P, Heath D. Performance of high-strength concrete walls exposed to fire. Adv Struct Eng 2018;21:1173–82.

[4] Ngo T, Fragomeni S, Mendis P, Ta B. Testing of Normal-and High-Strength Concrete Walls Subjected to Both Standard and Hydrocarbon Fires. ACI Struct J 2013;110.

[5] Ngo T, Mendis P, Whittaker A. A rate dependent stress-strain relationship model for normal, high and ultra-high strength concrete. Int J Prot Struct 2013;4:451–66.

[6] Popa M, Kiss Z, Constantinescu H, Bolca G. Case Study: Designing a 40 Storey High Office Building Using two Variants, with Regular Concrete Columns and with Compound Ultra-High Performance Concrete Columns and Regular Concrete Columns. Procedia Technol 2016;22:40–7.

[7] Plotzitza A, Rabczuk T, Eibl J. Techniques for numerical simulations of concrete slabs for demolishing by blasting. J Eng Mech 2007;133:523–33.

[8] Papadakis VG, Tsimas S. Supplementary cementing materials in concrete: Part I: efficiency and design. Cem Concr Res 2002;32:1525–32.

[9] Rupasinghe M, San Nicolas R, Mendis P, Sofi M, Ngo T. Investigation of strength and hydration characteristics in nano-silica incorporated cement paste. Cem Concr Compos 2017;80:17–30.

[10] Rupasinghe M, Mendis P, Ngo T, Nguyen TN, Sofi M. Compressive strength prediction of nano-silica incorporated

cement systems based on a multiscale approach. Mater Des 2017;115:379–92.

[11] Ni H-G, Wang J-Z. Prediction of compressive strength of concrete by neural networks. Cem Concr Res 2000;30:1245–50.

[12] Rabczuk T, Akkermann J, Eibl J. A numerical model for reinforced concrete structures. Int J Solids Struct 2005;42:1327–54.

[13] Rabczuk T, Belytschko T. Cracking particles: a simplified meshfree method for arbitrary evolving cracks. Int J Numer Methods Eng 2004;61:2316–43.

[14] Rabczuk T, Belytschko T. Application of particle methods to static fracture of reinforced concrete structures. Int J Fract 2006;137:19–49.

[15] Rabczuk T, Belytschko T. A three-dimensional large deformation meshfree method for arbitrary evolving cracks. Comput Methods Appl Mech Eng 2007;196:2777–99.

[16] Rabczuk T, Zi G, Bordas S, Nguyen-Xuan H. A geometrically non-linear three-dimensional cohesive crack method for reinforced concrete structures. Eng Fract Mech 2008;75:4740–58.

[17] Drzymała T, Jackiewicz-Rek W, Tomaszewski M, Kuś A, Gałaj J, Šukys R. Effects of high temperature on the properties of high performance concrete (HPC). Procedia Eng 2017;172:256–63.

[18] Zhao Y, Gong J, Zhao S. Experimental study on shrinkage of HPC containing fly ash and ground granulated blast-furnace slag. Constr Build Mater 2017;155:145–53.

[19] Erdal HI, Karakurt O, Namli E. High performance concrete compressive strength forecasting using ensemble models based on discrete wavelet transform. Eng Appl Artif Intell 2013;26:1246–54.

[20] Yeh I-C. Modeling of strength of high-performance concrete using artificial neural networks. Cem Concr Res 1998;28:1797–808.

[21] Lu S, Koopialipoor M, Asteris PG, Bahri M, Armaghani DJ. A Novel Feature Selection Approach Based on Tree Models for Evaluating the Punching Shear Capacity of Steel Fiber-Reinforced Concrete Flat Slabs. Materials (Basel) 2020;13:3902.

[22] Xu C, Gordan B, Koopialipoor M, Armaghani DJ, Tahir MM, Zhang X. Improving Performance of Retaining Walls Under Dynamic Conditions Developing an Optimized ANN Based on Ant Colony Optimization Technique. IEEE Access 2019;7:94692–700.

[23] Barkhordari MS, Armaghani DJ, Sabri MMS, Ulrikh DV, Ahmad M. The efficiency of hybrid intelligent models in predicting fiber-reinforced polymer concrete interfacial-bond strength. Materials (Basel) 2022;15:3019.

[24] Armaghani DJ, Skentou AD, Izadpanah M, Karoglou M, Khandelwal M, Konstantakatos G, et al. Deep neural networks for the estimation of granite materials' compressive strength using non-destructive indices. Appl. Artif. Intell. Mining, Geotech. Geoengin., Elsevier; 2024, p. 45–74.

[25] Asteris PG, Lourenço PB, Roussis PC, Adami CE, Armaghani DJ, Cavaleri L, et al. Revealing the nature of metakaolin-based concrete materials using artificial intelligence techniques. Constr Build Mater 2022;322:126500.

[26] Cavaleri L, Barkhordari MS, Repapis CC, Armaghani DJ, Ulrikh DV, Asteris PG. Convolution-based ensemble learning algorithms to estimate the bond strength of the corroded reinforced concrete. Constr Build Mater 2022;359:129504.

[27] Skentou AD, Bardhan A, Mamou A, Lemonis ME, Kumar G, Samui P, et al. Closed-Form Equation for Estimating Unconfined Compressive Strength of Granite from Three Non-destructive Tests Using Soft Computing Models. Rock Mech Rock Eng 2023;56:487–514.

[28] Koopialipoor M, Noorbakhsh A, Noroozi Ghaleini E, Jahed Armaghani D, Yagiz S. A new approach for estimation of rock brittleness based on non-destructive tests. Nondestruct Test Eval 2019:1–22.

[29] Tang D, Gordan B, Koopialipoor M, Jahed Armaghani D, Tarinejad R, Thai Pham B, et al. Seepage Analysis in Short Embankments Using Developing a Metaheuristic Method Based on Governing Equations. Appl Sci 2020;10:1761.

[30] Huang J, Koopialipoor M, Armaghani DJ. A combination of fuzzy Delphi method and hybrid ANN-based systems to forecast

ground vibration resulting from blasting. Sci Rep 2020;10:1–21.

[31] Huang L, Asteris PG, Koopialipoor M, Armaghani DJ, Tahir MM. Invasive weed optimization technique-based ANN to the prediction of rock tensile strength. Appl Sci 2019;9:5372.

[32] Momeni E, He B, Abdi Y, Armaghani DJ. Novel Hybrid XGBoost Model to Forecast Soil Shear Strength Based on Some Soil Index Tests. C Model Eng Sci 2023;136.

[33] Jafari MM, Jahandari S, Ozbakkaloglu T, Rasekh H, Jahed Armaghani D, Rahmani A. Mechanical properties of polyamide fiber-reinforced lime–cement concrete. Sustainability 2023;15:11484.

[34] Farahani HZ, Farahani A, Fakharian P, Jahed Armaghani D. Experimental Study on Mechanical Properties and Durability of Polymer Silica Fume Concrete with Vinyl Ester Resin. Materials (Basel) 2023;16.

[35] Barkhordari MS, Barkhordari MM, Armaghani DJ, Rashid ASA, Ulrikh DV. Hybrid wavelet scattering network-based model for failure identification of reinforced concrete members. Sustainability 2022;14:12041.

[36] Chou J-S, Pham A-D. Enhanced artificial intelligence for ensemble approach to predicting high performance concrete compressive strength. Constr Build Mater 2013;49:554–63.

[37] Prasad BKR, Eskandari H, Reddy BVV. Prediction of compressive strength of SCC and HPC with high volume fly ash using ANN. Constr Build Mater 2009;23:117–28.

[38] Naderpour H, Rafiean AH, Fakharian P. Compressive strength prediction of environmentally friendly concrete using artificial neural networks. J Build Eng 2018;16:213–9.

[39] Behnood A, Behnood V, Gharehveran MM, Alyamac KE. Prediction of the compressive strength of normal and high-performance concretes using M5P model tree algorithm. Constr Build Mater 2017;142:199–207.

[40] Hamdia KM, Lahmer T, Nguyen-Thoi T, Rabczuk T. Predicting the fracture toughness of PNCs: A stochastic approach based on ANN and ANFIS. Comput Mater Sci 2015;102:304–13.

[41] Mosavi A, Rabczuk T, Varkonyi-Koczy AR. Reviewing the novel machine learning tools for materials design. Int. Conf. Glob. Res. Educ., Springer; 2017, p. 50–8.

[42] Nazari A, Sanjayan JG. Modelling of compressive strength of geopolymer paste, mortar and concrete by optimized support vector machine. Ceram Int 2015;41:12164–77.

[43] Chou J-S, Chong WK, Bui D-K. Nature-inspired metaheuristic regression system: programming and implementation for civil engineering applications. J Comput Civ Eng 2016;30:4016007.

[44] Ibrahim IA, Khatib T. A novel hybrid model for hourly global solar radiation prediction using random forests technique and firefly algorithm. Energy Convers Manag 2017;138:413–25.

[45] Tzanetos A, Dounias G. Sonar inspired optimization (SIO) in engineering applications. Evol Syst 2020;11:531–9.

[46] Konstantinou C, Tzanetos A, Dounias G. Cardinality constrained portfolio optimization with a hybrid scheme combining a Genetic Algorithm and Sonar Inspired Optimization. Oper Res 2022;22:2465–87.

[47] Tzanetos A, Dounias G. Sonar inspired optimization in energy problems related to load and emission dispatch. Learn. Intell. Optim. 13th Int. Conf. LION 13, Chania, Crete, Greece, May 27–31, 2019, Revis. Sel. Pap. 13, Springer; 2020, p. 268–83.

[48] Yuan Z, Wang L-N, Ji X. Prediction of concrete compressive strength: Research on hybrid models genetic based algorithms and ANFIS. Adv Eng Softw 2014;67:156–63.

[49] Behnood A, Olek J, Glinicki MA. Predicting modulus elasticity of recycled aggregate concrete using M5′ model tree algorithm. Constr Build Mater 2015;94:137–47.

[50] Rebouh R, Boukhatem B, Ghrici M, Tagnit-Hamou A. A practical hybrid NNGA system for predicting the compressive strength of concrete containing natural pozzolan using an evolutionary structure. Constr Build Mater 2017;149:778–89.

[51] Sobhani J, Najimi M, Pourkhorshidi AR, Parhizkar T. Prediction of the compressive strength of no-slump concrete: A comparative study of regression, neural network and ANFIS models. Constr Build Mater 2010;24:709–18.

[52] Dogan G, Arslan MH, Ceylan M. Concrete compressive strength detection using image processing based new test method. Measurement 2017;109:137–48.

[53] Thomas RJ, Peethamparan S. Stepwise regression modeling for compressive strength of alkali-activated concrete. Constr Build Mater 2017;141:315–24.

[54] Onyelowe KC, Ebid AM, Mahdi HA, Riofrio A, Rezazadeh Eidgahee D, Baykara H, et al. Optimal Compressive Strength of RHA Ultra-High-Performance Lightweight Concrete (UHPLC) and Its Environmental Performance Using Life Cycle Assessment. Civ Eng J 2022;8:2391–410.

[55] Onyelowe KC, Eidgahee DR, Jahangir H, Aneke FI, Nwobia LI. Forecasting Shear Parameters, and Sensitivity and Error Analyses of Treated Subgrade Soil. Transp Infrastruct Geotechnol 2022.

[56] Jahangir H, Rezazadeh Eidgahee D. A new and robust hybrid artificial bee colony algorithm – ANN model for FRP-concrete bond strength evaluation. Compos Struct 2021;257:113160.

[57] Mojtahedi FF, Ahmadihosseini A, Eidgahee DR, Rezaee M, Spagnoli G. Bio-inspired Predictive Models Development for Strength Characterization of Cement Deep-Mixed Plastic Soils. Int J Geosynth Gr Eng 2024;10:1–22.

[58] Ahmadi M, Ebadi-Jamkhaneh M, Dalvand A, Rezazadeh Eidgahee D. Hybrid bio-inspired metaheuristic approach for design compressive strength of high-strength concrete-filled high-strength steel tube columns. Neural Comput Appl 2024;4.

[59] Shakouri Mahmoudabadi N, Bahrami A, Saghir S, Ahmad A, Iqbal M, Elchalakani M, et al. Effects of eccentric loading on performance of concrete columns reinforced with glass fiber-reinforced polymer bars. Sci Rep 2024;14:1890.

[60] Wei D, Zhang N, Jiao Y, Fan Y, Yu H, Koochakianfard O. Magneto-hygro-thermo-mechanical vibration analysis of spinning nanobeams with axisymmetric cross-sections incorporating surface, rotary inertia, and thickness effects. Eng Struct 2024;305:117702.

[61] Mozafarjazi M, Rabiee R. Experimental and numerical study on the load-bearing capacity, ductility and energy absorption of RC shear walls with opening containing zeolite and silica fume. Eng Solid Mech 2024.

[62] Zafar MS, Bakhshi A, Hojati M. Printability and shape fidelity evaluation of self-reinforced engineered cementitious composites. Constr Build Mater 2023;408:133676.

[63] Bakhshi A. Additive manufacturing of engineered cemen turing of engineered cementitious composi composites with ultra-high tensile ductility. New Mexico, 2023.

[64] Fang Z, Qajar J, Safari K, Hosseini S, Khajehzadeh M, Nehdi ML. Application of Non-Destructive Test Results to Estimate Rock Mechanical Characteristics—A Case Study. Minerals 2023;13:472.

[65] Kontoni D-PN, Onyelowe KC, Ebid AM, Jahangir H, Rezazadeh Eidgahee D, Soleymani A, et al. Gene Expression Programming (GEP) Modelling of Sustainable Building Materials including Mineral Admixtures for Novel Solutions. Mining 2022;2:629–53.

[66] Erdal HI. Two-level and hybrid ensembles of decision trees for high performance concrete compressive strength prediction. Eng Appl Artif Intell 2013;26:1689–97.

[67] Yuvaraj P, Murthy AR, Iyer NR, Sekar SK, Samui P. Support vector regression based models to predict fracture characteristics of high strength and ultra high strength concrete beams. Eng Fract Mech 2013;98:29–43.

[68] Lee A, Geem ZW, Suh K-D. Determination of optimal initial weights of an artificial neural network by using the harmony search algorithm: application to breakwater armor stones. Appl Sci 2016;6:164.

[69] Alavi AH, Gandomi AH. Prediction of principal ground-motion parameters using a hybrid method coupling artificial neural networks and simulated annealing. Comput Struct 2011;89:2176–94.

[70] Chang Y-T, Lin J, Shieh J-S, Abbod MF. Optimization the initial weights of artificial neural networks via genetic algorithm applied to hip bone fracture prediction. Adv Fuzzy Syst 2012;2012.

[71] Liu Q, Cui X, Chou Y-C, Abbod MF, Lin J, Shieh J-S. Ensemble artificial neural networks applied to predict the key risk factors of hip bone fracture for elders.

Biomed Signal Process Control 2015;21:146–56.

[72] Moghaddam TB, Soltani M, Shahraki HS, Shamshirband S, Noor NBM, Karim MR. The use of SVM-FFA in estimating fatigue life of polyethylene terephthalate modified asphalt mixtures. Measurement 2016;90:526–33.

[73] Kazemivash B, Moghaddam ME. A predictive model-based image watermarking scheme using Regression Tree and Firefly algorithm. Soft Comput 2018;22:4083–98.

[74] Lim C-H, Yoon Y-S, Kim J-H. Genetic algorithm in mix proportioning of high-performance concrete. Cem Concr Res 2004;34:409–20.

[75] Yeh I. Modeling slump of concrete with fly ash and superplasticizer. Comput Concr 2008;5:559–72.

[76] Videla C, Gaedicke C. Modeling Portland blast-furnace slag cement high-performance concrete. Mater J 2004;101:365–75.

[77] Pala M, Özbay E, Öztaş A, Yuce MI. Appraisal of long-term effects of fly ash and silica fume on compressive strength of concrete by neural networks. Constr Build Mater 2007;21:384–94.

[78] Siddique R, Aggarwal P, Aggarwal Y. Prediction of compressive strength of self-compacting concrete containing bottom ash using artificial neural networks. Adv Eng Softw 2011;42:780–6.

[79] de Graft-Johnson JWS, Bawa NS. Effect of mix proportion, water-cement ratio, age and curing conditions on the dynamic modulus of elasticity of concrete. Build Sci 1969;3:171–7.

[80] Vu-Bac N, Lahmer T, Zhuang X, Nguyen-Thoi T, Rabczuk T. A software framework for probabilistic sensitivity analysis for computationally expensive models. Adv Eng Softw 2016;100:19–31.

[81] Hamdia KM, Silani M, Zhuang X, He P, Rabczuk T. Stochastic analysis of the fracture toughness of polymeric nanoparticle composites using polynomial chaos expansions. Int J Fract 2017;206:215–27.

[82] Lee S, Ha J, Zokhirova M, Moon H, Lee J. Background information of deep learning for structural engineering. Arch Comput Methods Eng 2018;25:121–9.

[83] Pham BT, Nguyen MD, Nguyen-Thoi T, Ho LS, Koopialipoor M, Kim Quoc N, et al. A novel approach for classification of soils based on laboratory tests using Adaboost, Tree and ANN modeling. Transp Geotech 2021;27:100508.

[84] Yu H, Wilamowski BM. Levenberg-marquardt training. Ind Electron Handb 2011;5:1.

[85] Marquardt DW. An Algorithm for Least-Squares Estimation of Nonlinear Parameters. J Soc Ind Appl Math 1963;11:431–41.

[86] Levenberg K. A method for the solution of certain non-linear problems in least squares. Q Appl Math 1944;2:164–8.

[87] Wilamowski BM, Yu H. Neural network learning without backpropagation. IEEE Trans Neural Networks 2010;21:1793–803.

[88] Tzanetos A, Dounias G. A new metaheuristic method for optimization: sonar inspired optimization. Int. Conf. Eng. Appl. Neural Networks, Springer; 2017, p. 417–28.

[89] Lurton X. An introduction to underwater acoustics: principles and applications. Springer Science & Business Media; 2002.

[90] Nilsson M, Snoad N. Optimal mutation rates in dynamic environments. Bull Math Biol 2002;64:1033–43.

[91] Christopher M. Bishop. Pattern Recognition and Machine Learning (Information Science and Statistics). Springer 2006.

[92] Kohavi R. A study of cross-validation and bootstrap for accuracy estimation and model selection. Ijcai, vol. 14, Montreal, Canada; 1995, p. 1137–45.

[93] Badawy MF, Msekh MA, Hamdia KM, Steiner MK, Lahmer T, Rabczuk T. Hybrid nonlinear surrogate models for fracture behavior of polymeric nanocomposites. Probabilistic Eng Mech 2017;50:64–75.

[94] Hsu C-W, Chang C-C, Lin C-J. A practical guide to support vector classification 2003.

[95] Gandomi AH, Alavi AH, Shadmehri DM, Sahab MG. An empirical model for shear capacity of RC deep beams using genetic-simulated annealing. Arch Civ Mech Eng 2013;13:354–69.

[96] Mousavi SM, Aminian P, Gandomi AH, Alavi AH, Bolandi H. A new predictive model for compressive strength of HPC using gene expression programming. Adv Eng Softw 2012;45:105–14.